International Journal of Modern Physics A
Vol. 36, Nos. 11 & 12 (2021) 2140002 (11 pages)

DOI: 10.1142/S0217751X21400029

Exploration of the coupling between thrust and interference in Taiji-1

Juan Wang, Ran Yang* and Yu Niu†

Center for Gravitational Wave Experiment, National Microgravity Laboratory, Institute of Mechanics, Chinese Academy of Sciences (CAS), Beijing 100190, P. R. China

Taiji Laboratory for Gravitational Wave Universe (Beijing/Hangzhou), University of Chinese Academy of Sciences (UCAS), Beijing 100049, P. R. China

*yangran@imech.ac.cn
†*niuyu@imech.ac.cn*

‡*On behalf of The Taiji Scientific Collaboration*

Received 15 September 2020
Revised 16 October 2020
Accepted 30 October 2020
Published 27 February 2021

As the first technology verification satellite of the space-based gravitational wave detection in China, Taiji-1 has tested the high-precision space laser interferometer, the inertial sensor, the micro thruster and the hyperstatic satellite platform in orbit. The micro thruster plays an important role in the micro propulsion system. The purposes of the research are to investigate the relationship between the thrust and the interference, and then get a comprehensive understanding about the maximum effect of the thrust in Taiji-1. The transfer function between the thrust and the optical path difference fluctuations is established through the modeling, the simulation and the data postprocessing of Taiji-1. In addition, the maximum effect of the thrust in Taiji-1 is about 32 pm/$\sqrt{\text{Hz}}$ with an integration time of 100 s. It can be neglected compared to the requirement of 100 pm/$\sqrt{\text{Hz}}$ for the interferometer stability in Taiji-1.

Keywords: Force noise analysis; thrust; optical path analysis; numerical simulation.

1. Introduction

Since the discovery of the gravitational waves (GWs) by American LIGO in 2016, the space-based GW detection has become the major focus in the next stage of GW astronomy.[1,2] Taiji program, space-based GW detection in China,[3,4] is based

*,†Corresponding authors.
‡For more details, please refer to article 2102002 of this Special Issue.

on a triangle of three spacecrafts, with 3 million kilometers between them, in orbit around the sun. It is claimed to be launched in 2033. The measurement requirement of Taiji program, based on the laser heterodyne interference, is set to reach the order of $1\,\mathrm{pm}/\sqrt{\mathrm{Hz}}$ with frequencies region between 0.1 mHz and 1 Hz.[5–7] As the first technology experimental satellite for Taiji program, Taiji-1 has carried out the technical validation of many key technologies in orbit, such as the high-precision space laser interferometer, the inertial sensor, the micro thruster and the hyperstatic satellite platform. In particular, the measurement sensitivity of the interferometer is set to achieve $100\,\mathrm{pm}/\sqrt{\mathrm{Hz}}$ covering the range from 10 mHz to 1 Hz. Besides, the drag-free control system has been validated in orbit for the first time in China, which detects the position fluctuation of the test mass through the inertial sensor, and then keeps the satellite centered with respect to the test mass by the micro thruster.

To reach the future measurement requirement of Taiji program, it is necessary to analyze the effect of each possible noise sources. Many researches have been done to analyze the effect of noise sources on the interferometer, such as the frequency noise of the pre-stabilized laser, the disturbance caused by nonconservative force and the noise coming from the drag free control algorithm, etc.[8] However, the effect of micro thruster on the sensitivity of the interferometer has not been described. As the actuator for the drag-free system,[9,10] the micro thruster provides the maximum thrust of 50 μN, which will transmit into the optical bench through the structure of the satellite and have an influence on the interference. The relationship between the thrust and the interference is investigated in this research to analyze the effect of the thrust and remove the force noise from the interference results further.

Because the structure of the satellite is complicated, it is difficult to give the relationship between the thrust and the interference by theoretical studies. Furthermore, to get the maximum effect and transmission mechanism of the thrust, the integrated analysis of mechanics and optics has been proposed. Firstly, the satellite is mechanically modeled. Then by the mechanical simulation of the model, the deformation of the optical bench caused by the thrust is available, and the corresponding optical path difference (OPD) fluctuations can be obtained through the optical simulation of the interference optical path. Moreover, the transfer function between the thrust and the OPD fluctuations is established by data postprocessing. Finally, the maximum effect of the thrust on the interference results in Taiji-1 can be derived from the transfer function.

2. The Numerical Simulation of Taiji-1

2.1. *The finite element model of Taiji*-1

The numerical simulation of Taiji-1 is necessary considering that Taiji-1 model is sophisticated. However, to get the precise results by simulation is still a challenge. Accordingly, the appropriately simplified model of Taiji-1, as precondition of the reliable simulation, is used to analyze the transmission mechanism of the thrust. It is important to have an understanding of the structure, the materials and the

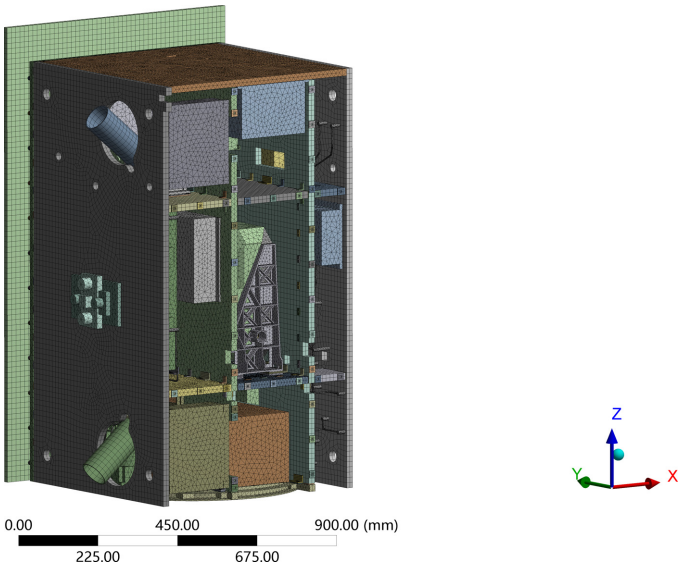

Fig. 1. The finite element model of Taiji-1.

properties of the whole satellite, which will be used to simplify the model, set connection conditions and mesh.

The main components of Taiji-1 are the micro thrusters, the support structure, the electronic devices and the optical bench, which is located in the central area of the satellite. To simplify the satellite properly, the materials related to the model are set to be linear and isotropic. Besides, some simplified methods have been adopted. For instance, the electronic devices have been replaced by the solid boxes with the same mass.

More than 600 bodies exist in the model and the size of each body has a big difference. In order to facilitate the quality of the mesh and further improve the validity of the modeling, it is necessary to classify the bodies and to mesh in different sizes. As shown in Fig. 1, there are 8,74,555 grids in this finite element model.

2.2. *The mechanical simulation of Taiji-1*

The real operating conditions of Taiji-1 need to be reproduced during the mechanical simulation. This can be achieved by the proper analysis settings, especially the conditions for the application of the constraints. Because the satellite is always in a state of free falling in space, the model is not subject to any constraint. Besides, as previously stated, the micro thrusters keep the satellite centered with respect to the test mass, so the thrust applied on the assigned area is varied over time. Consequently, transient dynamics is used to analyze the effect of the time-varied thrust on the response deformation, since the transient dynamics can be used to analyze the displacement, the stress and the strain caused by the time-varied load.

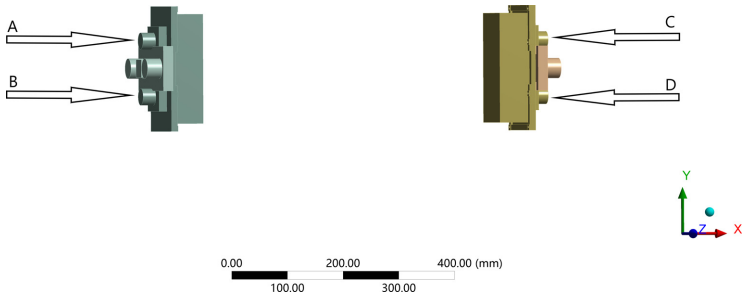

Fig. 2. Diagram of the thrust application.

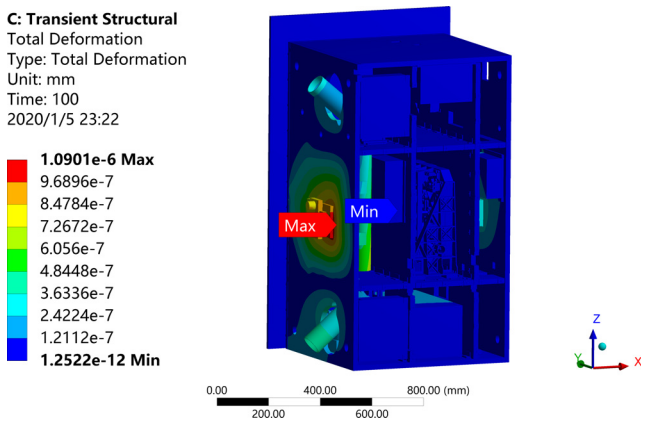

Fig. 3. The deformation of the whole satellite.

Although four sets of micro thrusters are arranged, the situation related to two sets of them, which is the real operating condition in Taiji-1, is discussed in this research as shown in Fig. 2. Assuming the applied time-varied thrust is

$$F = F_0 \cdot \sin\left(\frac{2\pi}{T} \cdot t\right), \tag{1}$$

where F_0 is the amplitude and T represents the period of the thrust.

The analysis parameters are set to be 200 s for the duration time of the thrust, 10 s for the period of the thrust. Then the deformation of the optical bench used for the following optical simulation can be derived by transient dynamics. For example, the thrust applied on the left or the right set of the micro thrusters is shown in Eq. (2). The corresponding deformation diagram of the whole satellite and the optical bench are shown in Figs. 3 and 4, respectively.

$$\begin{aligned} F_{A,B} &= 2 \cdot \sin(0.2\pi \cdot t), \\ F_{C,D} &= 1 \cdot \sin(0.2\pi \cdot t). \end{aligned} \tag{2}$$

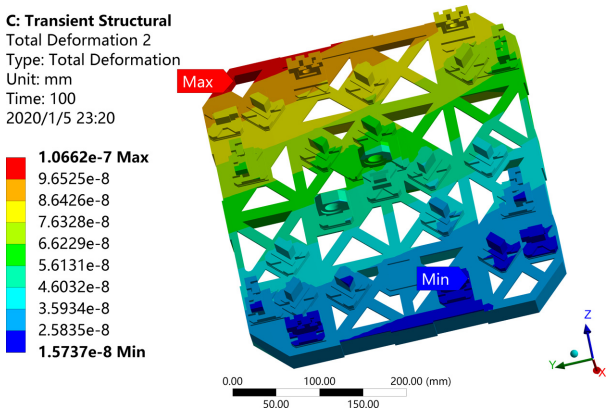

Fig. 4. The deformation of the optical bench.

It is shown that the optical elements on the optical bench are deformed in different degrees, and the deformation data of the optical elements at each moment can be derived.

2.3. *The optical simulation of the interference optical path*

The interference optical path is changed since the optical elements on the optical bench are deformed. To reproduce the interference optical path and get the fluctuation of the OPD, the optical simulation is implemented. The layout of the optical path in Taiji-1 is shown in Fig. 5. In this design, the laser at 1064 nm with waist

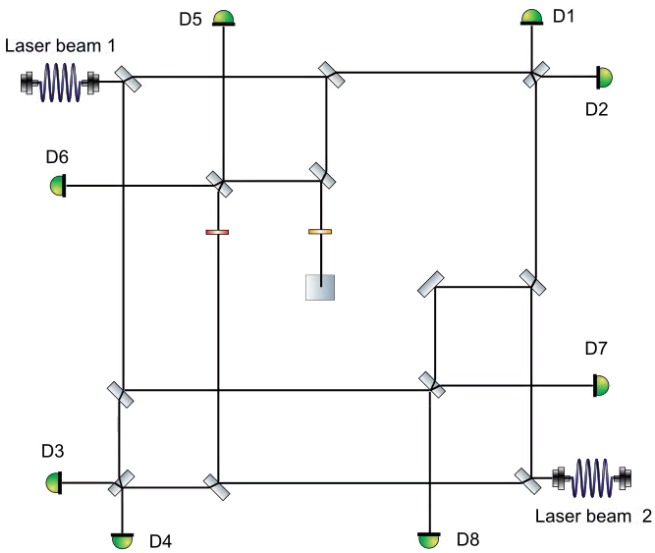

Fig. 5. The layout of the optical path in Taiji-1.

about 0.5 mm is delivered from Nd:YAG laser, and passes the fiber optic splitter, the acousto-optic modulator (AOM), the collimator and other optical lenses in turn. Through the splitter and the AOM, the laser is divided into the laser beams 1 and 2 of equal intensity with a frequency difference of 1 KHz.

It is shown that four interferometric signals are formed and transformed into electrical signals by photodetectors at the end of each interference path. Eight detectors are classified into four groups: detectors 1 and 2, detectors 3 and 4, detectors 5 and 6, detectors 7 and 8. The detectors of each group make backups for each other, which means the changes of the measured OPD are equal in each group within the accuracy range of the detectors. One of the interference path is related to a central triangular reflecting prism. The incident light is reflected by this prism to the test mass and back again. The light path between the triangular reflecting prism and the test mass is vertical to the optical bench.

The reproduction of the interference optical paths can be realized by the optical software. Firstly, the node coordinates of the optical elements can be obtained based on the initial coordinates and the deformation derived from the simulation of mechanics. The node coordinates can be fitted to a surface, and a third-order face fitting is used here. Then the interference optical paths are simulated. Finally, the OPD data for four interference optical paths at each moment can be exported.

3. Results and Analysis

To investigate the influence of the thrust, the postprocessing of interference optical path data at each moment is carried out to explore the coupling between the thrust and the interference. As previously pointed out, the whole model can be seen as a linear system. In a linear system, the steady-state response to the harmonic excitation is still a harmonic vibration, with the same frequency and the phase lags behind the excitation, according to the theory of vibration mechanics.[11] To simplify the analysis process, the system damping is not considered, and it leads the phase lag caused by vibration of the structure to be zero. It means that the frequency and the phase of the interference results are the same as those of the applied thrust. Therefore, the amplitude of both the OPD fluctuations and the thrust is mainly considered in the following analysis.

3.1. *The analysis of the optical path difference fluctuations*

The OPD data for a duration time of 100 s have been obtained by the former simulation. Analysis of these data under different conditions can make a preparation for the establishment of the transfer function. For example, a thrust of 0.02 N with a period of 10 s is applied on the left set of the micro thrusters, and the changes in the OPD over time in eight detectors are shown in Fig. 6. As a contrast, the corresponding changes are shown in Fig. 7 when a thrust with the amplitude of 0.01 N is applied on the right set of the micro thrusters.

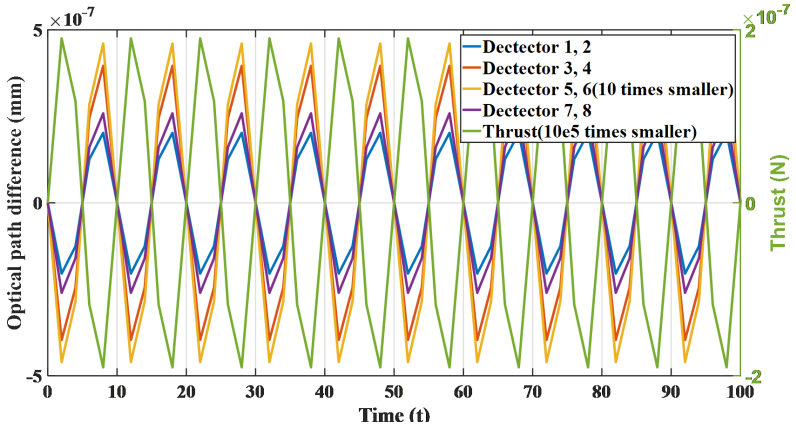

Fig. 6. Diagram of changes in OPD over time caused by the left set of thrusters.

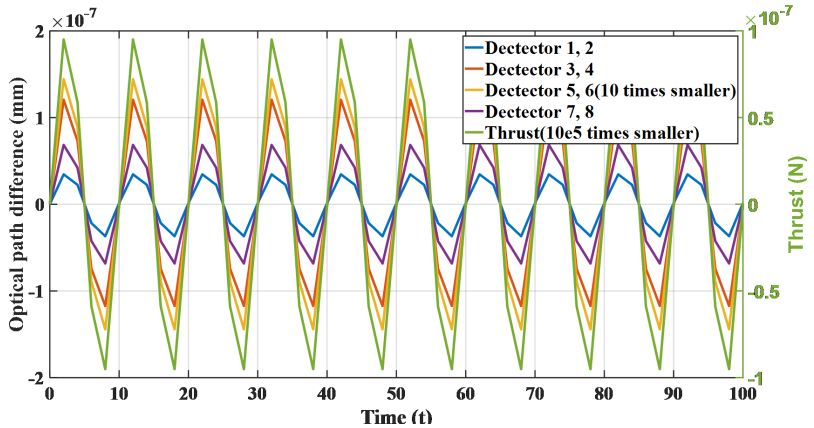

Fig. 7. Diagram of changes in OPD over time caused by the right set of thrusters.

It is shown that the OPD fluctuation is nearly a sine function corresponding to time, and the period of the thrust is the same as that of the OPD. It is in agreement with the theoretical prediction. At the same time, the phase difference of π between the thrust and the OPD is shown in Fig. 6. However, the phase difference is zero in Fig. 7. The explanation to this phenomenon is that the two different thrusts are applied on the opposite directions.

3.2. *The establishment of the transfer function*

To get the responses of the arbitrary thrust, the establishment of the transfer function between the thrust and the interference is necessary. Due to the small number of data samples and the requirement to increase the accuracy of analysis, a fast

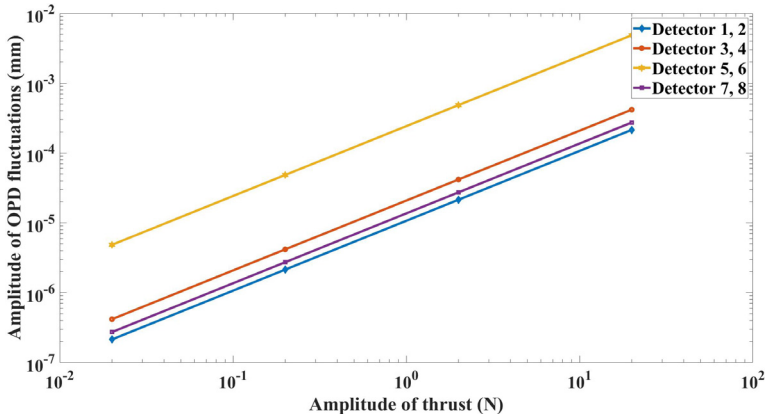

Fig. 8. The relationship between the amplitude of OPD fluctuations and the amplitude of thrust.

Fourier transform (FFT) is performed to take the amplitude-frequency characteristics of the OPD fluctuations. By extracting the information of the amplitude, the relationship between the amplitude of the OPD fluctuations and the amplitude of the thrust can be observed.

On the one hand, the amplitudes of the thrust applied on the left set of the micro thrusters are 0.02, 0.2, 2 and 20 N, respectively, with a period of 10 s. The relationship between the amplitude of OPD fluctuations and the amplitude of the thrust is presented on a logarithmic scale, as shown in Fig. 8.

It is discovered that the amplitude of the OPD fluctuations is linear with respect to the amplitude of the thrust, and the coefficients of the linearity are different for each interference optical path. The numerical relationships between them are shown in Eq. (3).

$$\begin{aligned} D_{1,2} &= 1.070\times10^{4}\cdot F(\text{pm}),\\ D_{3,4} &= 2.084\times10^{4}\cdot F(\text{pm}),\\ D_{5,6} &= 2.422\times10^{5}\cdot F(\text{pm}),\\ D_{7,8} &= 1.365\times10^{4}\cdot F(\text{pm}). \end{aligned} \tag{3}$$

On the other hand, the amplitudes of thrust applied on the right set of the micro thrusters are 0.01, 0.1, 1 and 10 N, respectively, with a period of 10 s. The corresponding relationships can be shown in Eq. (8) by the same procedure.

$$\begin{aligned} D_{1,2} &= 3.753\times10^{3}\cdot F(\text{pm}),\\ D_{3,4} &= 1.251\times10^{4}\cdot F(\text{pm}),\\ D_{5,6} &= 1.517\times10^{5}\cdot F(\text{pm}),\\ D_{7,8} &= 7.192\times10^{3}\cdot F(\text{pm}). \end{aligned} \tag{4}$$

To get closer to the actual operating conditions, it is also important to consider the OPD fluctuations caused by the thrust, applied on both sets of micro thrusters.

Table 1. The amplitudes of the OPD fluctuations in three cases.

Detectors	0.02 N (left set only) (pm)	0.01 N (right set only) (pm)	0.02 N (left) and 0.01 N (right) (pm)
1, 2	$D_L = 214$	$D_R = 37.53$	$D = 176.4$
3, 4	$D_L = 416.7$	$D_R = 125.1$	$D = 291.6$
5, 6	$D_L = 4843$	$D_R = 1517$	$D = 3326$
7, 8	$D_L = 272.9$	$D_R = 71.92$	$D = 201$

For example, the sinusoidal thrust of 0.02 N is applied on the left set and 0.01 N with the same period of 10 s is applied on the right set of micro thrusters, simultaneously. By contrast, the results of 0.02 N applied on the left set only or 0.01 N applied on the right set only can be obtained in Eq. (3) or Eq. (4). The amplitudes of the OPD fluctuations corresponding to these three cases are listed in Table 1.

For these cases, we can approximately obtain

$$D = D_L - D_R, \tag{5}$$

which means the interference result caused by thrust applied on both sets of micro thrusters is a linear superposition of the results by the thrust applied on the one set only.

Combining the linear superposition expressed in Eq. (5) and phase difference of π or 0 shown in Fig. 6 or Fig. 7, the final transfer function between the thrust and the interference results can be expressed as follows:

$$\begin{aligned} D_{1,2} &= |-1.070\times10^4\cdot F_L + 3.753\times10^3\cdot F_R|(\text{pm}),\\ D_{3,4} &= |-2.084\times10^4\cdot F_L + 1.251\times10^4\cdot F_R|(\text{pm}),\\ D_{5,6} &= |-2.422\times10^5\cdot F_L + 1.517\times10^5\cdot F_R|(\text{pm}),\\ D_{7,8} &= |-1.365\times10^4\cdot F_L + 7.192\times10^3\cdot F_R|(\text{pm}). \end{aligned} \tag{6}$$

It can be also seen that the amplitude of the OPD fluctuations in detectors 5 and 6 is an order of magnitude higher than those in other detectors. One reason for this phenomenon is that the light path detected by detectors 5 and 6 are concentrated on the area with the greatest deformation of the interferometer. The other reason is that the light path detected by detectors 5 and 6 passes through the triangular reflecting prism and the test mass. Thus, the interference results contain the change of OPD between the prism and the test mass, which does not exist in other optical paths.

3.3. *The maximum effect of the thrust in Taiji-1*

Since the transfer function has been established, the next purpose of the research is to explore the maximum effect of the thrust with μN magnitude. The interference result is proportional to the thrust applied on the micro thrusters as expressed in Eq. (6). As a result, when the maximum thrust of 50 μN is applied on both sets of micro thrusters in Taiji-1, the amplitude of the OPD fluctuations based on the

transfer function can be given as

$$\begin{aligned} D_{1,2} &= 0.347 \text{ (pm)}, \\ D_{3,4} &= 0.417 \text{ (pm)}, \\ D_{5,6} &= 4.525 \text{ (pm)}, \\ D_{7,8} &= 0.323 \text{ (pm)}. \end{aligned} \tag{7}$$

In the time domain, the maximum response amplitude of the OPD fluctuations is 4.525 pm in detectors 5 and 6. To be consistent with the noise analysis method used in Taiji-1, the amplitude spectrum density (ASD) analysis with respect to the integration time is needed. With an integration time of 100 s, the corresponding maximum ASD of the interference result is[12]

$$\text{ASD} = (A \cdot \sqrt{T})/\sqrt{2} = (4.525 \times \sqrt{100})/\sqrt{2} = 32(\text{pm}/\sqrt{\text{Hz}}). \tag{8}$$

4. Conclusion

In this paper, the integrated analysis of mechanics and optics has been used to explore the coupling between the thrust and the interference in Taiji-1. First, through the modeling, the simulation and the data postprocessing, the transfer function between the thrust and the OPD fluctuations is established. It can be discovered that the amplitude of the OPD fluctuations is linear with respect to the amplitude of the thrust, and the coefficients of the linearity are different for each interference optical path. Second, the transfer function has indicated that the maximum effect of thrust is about 32 pm/$\sqrt{\text{Hz}}$ with an integration time of 100 s. In this situation, the effect is not significant and can be ignored when compared to the interferometer stability of 100 pm/$\sqrt{\text{Hz}}$ in Taiji-1. It should be noticed that the maximum effect of the thrust is related to the integration time.

For future Taiji program, with the measurement requirement up to the order of 1 pm/$\sqrt{\text{Hz}}$ and the increasing integration time, the force noise caused by the micro thrusters will not be ignored. The research in this paper is just a preliminary attempt to establish a quantitative relationship between the thrust and the interference. For a more detailed force noise analysis, the next step of experiments and analysis is needed to verify and revise the coupling relationship.

Acknowledgments

This work was financially supported by the Strategic Priority Research Program of the Chinese Academy of Sciences (Grant Nos. XDA1502070902, XDA1502070304 and XDA1501800003).

References

1. B. P. Abbott *et al.*, *Phys. Rev. Lett.* **116**, 061102 (2016).
2. M. Armano *et al.*, *Phys. Rev. Lett.* **120**, 061101 (2018).

3. Z. R. Luo *et al.*, *Opt. Laser Technol.* **105**, 146 (2018).
4. Z. R. Luo *et al.*, *Res. Phys.* **16**, 102918 (2020).
5. W. R. Hu and Y. L. Wu, *Natl. Sci. Rev.* **4**, 685 (2017).
6. Z. R. Luo, M. Zhang and G. Jin, *Chin. Sci. Bull.* **64**, 2468 (2019).
7. H. S. Liu *et al.*, *Microgravity Sci. Technol.* **30**, 775 (2018).
8. G. Jin, Program in space detection of gravitational wave in Chinese Academy of Sciences, in *11th Int. LISA Symp.*, Zurich, Switzerland, 2016.
9. X. M. Xu *et al.*, *Microsyst. Technol.* **23**, 5003 (2017), https://doi.org/10.1007/ s00542-017-3451-4
10. D. Tombolato, A laboratory study of force disturbances for the LISA Pathfinder free fall demonstration mission, Doctoral dissertation, Ph D. dissertation, University of Trento (2008).
11. X. T. Zhang *et al.*, *Mechanics of Structural Vibration*, 2nd edn. (Tongji University Press, Shanghai, 2005).
12. Y. H. Dong, Inter-satellite interferometry: Fine pointing and weak-light phase-locking techniques for space gravitational wave observatory, Doctoral dissertation, Ph D. dissertation, University of Chinese Academy of Sciences (2016).